Research Square

Preprints are preliminary reports that have not undergone peer review.
They should not be considered conclusive, used to inform clinical practice,
or referenced by the media as validated information.

In Silico Characterization of Desmodium gangeticum Compounds as Dual Modulators of MAO-B and 5- HT2A in Parkinson's Disease: An Integrated Approach Combining Molecular Docking, ADMET Profiling, MM-GBSA, QSAR Modeling, and Molecular Dynamics Simulation

Oluwabusayo Esther Akinma
Teady Bioscience Research Laboratory
Olufemi Adebisi Akinola
Federal University of Technology
Ifeoluwa Deborah Ojo
Teady Bioscience Research Laboratory
Akinyode Isaac Olopoda
akinyodeisaac15@gmail.com
Federal University of Technology
Ifedayo David Akerele
Teady Bioscience Research Laboratory
Bright Bayonle Akinyemi
Teady Bioscience Research Laboratory
Folashade O. Ayodeji
Teady Bioscience Research Laboratory
Olusola Olalekan Elekofehinti
Federal University of Technology

Research Article

Keywords: Parkinson, Monoamine Oxidase B, Characterization, Molecular Docking, Dopaminegic Neurone

Posted Date: July 10th, 2026

DOI: https://doi.org/10.21203/rs.3.rs-10242302/v1

License: This work is licensed under a Creative Commons Attribution 4.0 International License.
Read Full License

Additional Declarations: No competing interests reported.

Version of Record: A version of this preprint was published at In Silico Pharmacology on October 25th, 2026. See the published version at https://doi.org/10.1007/s40203-026-00773-7.

In Silico Characterization of *Desmodium gangeticum* Compounds as Dual Modulators of MAO-B and 5-HT2A in Parkinson's Disease: An Integrated Approach Combining Molecular Docking, ADMET Profiling, MM-GBSA, QSAR Modeling, and Molecular Dynamics Simulation

Oluwabusayo Esther Akinma[1], Olufemi Adebisi Akinola[1,2], Ifeoluwa Deborah Ojo[1], Akinyode Isaac Olopoda[1,2], Ifedayo David Akerele[1], Bright Bayonle Akinyemi[1], Folashade O. Ayodeji[1], Olusola Olalekan Elekofehinti[1,2]

1. Teady Bioscience Research Laboratory, Ilara-Mokin, Ondo State, Nigeria
2. Department of Biochemistry, Federal University of Technology, Akure, Nigeria

First Co-author: Oluwabusayo Esther Akinma (akinmabusayo1@gmail.com)

Corresponding Author: Akinyode Isaac Olopoda (akinyodeisaac15@gmail.com)

Abstract

Management of Parkinson's disease (PD) is challenging: dopaminergic treatments alleviate motor symptoms but exacerbate psychosis, while antipsychotics alleviate hallucinations but exacerbate motor symptoms. To tackle this problem, we combined the in-silico profiling of *Desmodium gangeticum's* phytochemicals with dual monoamine oxidase-B (MAO-B) and 5-hydroxytryptamine type 2A (5-HT2A) modulating activity. Docking studies suggested Desmodin and 5,7,2′,4′-Tetrahydroxy-6-prenylisoflavanone as potential MAO-B modulators and N, N-Dimethyltryptamine and Tryptamine as 5-HT2A modulators. ADMET profiling revealed promising central nervous system (CNS) drug-likeness, adequate blood-brain barrier penetration and tolerability. Toxicity prediction showed non-toxicity towards hepatotoxicity, mutagenicity and carcinogenicity. MM-GBSA calculations and molecular dynamics studies supported strong interactions and AutoQSAR indicated bioactivity. Thus, these findings indicate that metabolites of *D. gangeticum* are potentially effective bi-therapy molecules to treat the motor and neuropsychiatric symptoms of PD. These phytochemicals need experimental research to advance their development as safer and multi-targeted drug candidates for clinical trials.

Keywords: Parkinson; Monoamine Oxidase B; Characterization; Molecular Docking; Dopaminegic Neurone

Introduction

Parkinson's disease (PD) is a progressive, chronic neurodegenerative disease marked by selective and irreversible loss of dopaminergic neurons in the substantia nigra pars compacta, resulting in severe depletion of dopamine in the striatum and formation of Lewy bodies, mainly comprising α-synuclein (Schiess *et al.,* 2022). PD is the second most common neurodegenerative disorder and the third most serious health concern for middle-aged and elderly people, after cancer and cardiovascular disease (Segal *et al.,* 2021). PD has the fastest-growing incidence and disability of all neurological diseases (Schiess *et al*., 2022), with a global prevalence that increased from 2.5 million cases in 1990 to over 8.5 million cases in 2019 (Zhong and Zhu, 2022), and is projected to reach 25.2 million by 2050 due to population ageing (Su *et al.,* 2025). Clinically, PD symptoms are both motor and non-motor: the classic "tremor, rigidity, bradykinesia" motor triad, and postural instability are still the main diagnostic criteria, but non-motor complications, such as cognitive dysfunction, autonomic dysfunction, depression, sleep dysfunction, and neuropsychiatric symptoms, also represent a very disabling burden (Alborghetti *et al.,* 2023). One of the most debilitating non-motor symptoms is PD psychosis, which affects as many as 60% of patients and is characterised by hallucinations, delusions, illusions, and a sense of presence (Segal *et al.,* 2021). PD remains an incurable disease, and its progressive nature highlights the need for new, safer, and more effective treatment options (Schiess *et al.,* 2022).

The main pharmacological treatment for PD is dopamine replacement with levodopa, which is the most effective symptomatic therapy; but long-term use is associated with motor fluctuations and dyskinesia, so adjunct therapies are needed to improve quality of life (Di Biase *et al*., 2023; de Bie *et al*., 2025). These include monoamine oxidase type B (MAO-B) inhibitors (selegiline, rasagiline, safinamide), which stop the breakdown of dopamine, thereby alleviating motor symptoms such as akinesia and rigidity and potentially having neuroprotective properties (Tan *et al*., 2021; Alborghetti *et al*., 2023). However, MAO-B inhibitor therapy suffers from psychiatric side effects, including delirium, hallucinations and agitation, particularly for selegiline, which produces amphetamine-like metabolites (Jost, 2022). In addition, dopaminergic medications aggravate non-motor symptoms, with dopamine-induced psychosis (e.g., visual hallucinations) being a major impediment to the optimization of anti-Parkinsonian treatment, especially in elderly or advanced PD patients (Cummings *et al*., 2024). This therapeutic dilemma underscores the need for multifunctional drugs that do not abolish dopaminergic effects and counter dopamine-induced psychosis.

The serotonin system, and in particular, the 5-hydroxytryptamine type 2A (5-HT2A) receptor, is a key driver of neuropsychiatric complications in PD. Increasing evidence supports 5-HT2A's role in cognition and visual hallucinations, with hallucinations persisting after tapering or cessation of dopaminergic drugs (Kossatz *et al.,* 2024). Neurobiologically, PD psychosis has been proposed to be a serotonin-dopamine imbalance syndrome, resulting from an imbalance between these neurotransmitter systems in important neural circuits (Segal *et al.,* 2021). PD psychosis has been shown to respond to 5-HT2A blockade in Phase III clinical trials, highlighting the role of this target in its pathophysiology (Tariot *et al.,* 2021). This target was clinically validated in the approval of pimavanserin, a selective 5-HT2A inverse agonist, as the first FDA-approved medication to treat PD psychosis, which has been shown to improve hallucinations and delusions, while avoiding motor complications caused by D2 receptor blockade (Cummings *et al.,* 2024). But pimavanserin is contraindicated due to a black box warning for QTc prolongation and mortality in older adults with dementia-related psychosis (Torres-Yaghi *et al.,* 2021; Schneider, 2022). Thus, the challenge in managing PD psychosis is that dopaminergic agents exacerbate psychosis, while traditional antipsychotics create motor dysfunction. These drug interactions suggest the need for bifunctional agents that can maintain the beneficial effects of dopaminergic therapies while also blocking serotonin-associated psychosis, and modulating MAO-B and 5-HT2A represents an attractive hypothesis.

The global return to phytochemicals as a source of drug discovery is driven by the pharmacological limitations of existing synthetic drugs, as well as the evolutionary pre-optimization of plant chemicals for biological activity (Rahman *et al.,* 2021). Natural products have long been used in traditional medicine for their healing properties. Plants, marine organisms, and fungi contain diverse

secondary metabolites that play significant roles in many medicinal practices, offering antioxidant, anti-inflammatory, and neuroprotective effects that position them as promising alternatives to traditional drugs (de Lima *et al.,* 2025). Approximately 50% of clinically approved drugs have been derived from or inspired by natural scaffolds, and this proportion is particularly pronounced in the neurological space, where structurally complex phytochemicals can interact with multiple neurological targets simultaneously (Fakhri *et al.,* 2021). The structural mimicking of natural compounds to endogenous ligands has presented them as potential therapeutic candidates to prevent the development of neurodegenerative diseases, and multi-target natural products have shown promising success in drug discovery against these conditions (Sharifi-Rad *et al.,* 2022).

Desmodium gangeticum (L.) DC. (family Fabaceae), commonly known as Shalparni in the Ayurvedic tradition, represents a particularly compelling candidate for such investigation. *Desmodium gangeticum* has been used for treating various diseases and is one among ten ingredients of the classical Ayurvedic formulation Dasamula (Bora *et al.,* 2023). Decoctions of its root and leaf, root powder, and leaf juice are used as tonics, febrifuge, digestive, antiemetic, astringent, anti-asthmatic, antidiarrhoeal, and anti-inflammatory agents in the traditional medicinal practices of India and its neighbouring countries (Bora *et al.,* 2023). Phytochemical investigations have established the plant's remarkable chemical richness: the roots of *Desmodium gangeticum* are rich in alkaloids, terpenoids, steroids, flavonoids, phenylpropanoids, pterocarpans, volatile oil, coumarins, phenol, isoflavonoids, glycosides, pterocarpenoids, and saponins, and are the main ingredients of famous Ayurvedic preparations including Dasmularistha, Dasmulakwath, and Brahma Rasayana (Bora *et al.,* 2023). Major bioactive components of the plant, such as desmodin, gangetin, hordenine, kaempferol, quercetin, and tryptamine alkaloids, have been found to possess a wide range of pharmacological activities, including anti-inflammatory, antioxidant, anti-amnesic, and central nervous system (CNS) activities (Bora *et al.,* 2023; Mohan *et al.,* 2021). Cognitive- and neuroprotective-active compounds from *Desmodium gangeticum* have recently been evaluated as potential enzyme inhibitors in neurodegenerative diseases, such as BACE1, a key enzyme in Alzheimer's disease development. This inherent neurological activity, along with the plant's rich phytochemicals and excellent safety profile, offers solid mechanistic grounds for targeted screening against PD-related targets (Chang *et al.,* 2024).

Traditional drug discovery processes, from target identification to clinical trials, are costly, taking 10-15 years and involve spending more than US$800 million for each drug that is approved (Vemula *et al.,* 2022). This process has been revolutionised by computer-aided drug discovery (CADD), also known as in silico screening. The use of bioinformatics in drug discovery and development can drastically cut costs and shorten the time required for drug development, and computational approaches have been extensively used for high-throughput screening (Vemula *et al.,* 2022).

MATERIALS AND METHOD

Protein Preparation

The three-dimensional crystal structures of human monoamine oxidase-B (MAO-B) bound with safinamide (PDB ID: 2V5Z) and 5-Hydroxytryptamine receptor 2A (5-HT2A) (PDB ID: 6WGT) were downloaded from the RCSB Protein Data Bank, and then subjected to processing with the Protein Preparation Wizard tool in Maestro (Schrödinger, LLC. 2021; version 12.8) according to standard procedures in structure-based drug design (Sastry *et al.,* 2021). The protein structures were imported into Maestro one by one, and the Protein Preparation Wizard was used to prepare the proteins for docking. The wizard allows the user to view only polar hydrogen atoms, which makes it easier to understand the hydrogen bonding pattern.

The Protein Preparation Wizard is comprised of two main sections: preprocessing and refinement. During the preprocessing step, a number of important steps were carried out, including the assignment of bond orders, addition of missing hydrogens to ensure proper ionization, removal of crystallographic waters and solvents, and selection of desired protein chains and ligands while removing alternate chains. This stage also included protonation state correction for amino acids at physiological pH (7.4) to achieve the required ionization (Johnston *et al.,* 2023). During the refinement stage, hydrogen bond optimization was executed to achieve the correct geometry and improve the stability of the structure. An interactive hydrogen bond

optimization tool enabled selection and refinement of hydrogen-bonded clusters. Energy minimization was carried out using the OPLS4 force field until the average root mean square deviation (RMSD) of non-hydrogen atoms was reduced to 0.3 Å, to ensure that the protein structure was maintained in a stable and plausible conformation with minimal distortion (Lu *et al.,* 2021; Roos *et al.,* 2021).

Receptor Grid Generation

The receptor grid file was generated via Receptor Grid Generation panel by picking the co crystallized ligand located at the active site of the proteins to automatically supply x, y, and z coordinates (Ojo *et al.,* 2025). The coordinates for MAO-B are X: 55.87, Y: 142.96, and Z: 17.13, while those for 5-HT2A are X: 24.97, Y: 40.3, and Z: 54.47.

Ligand Preparation

After preparing the target proteins, a library of 37 bioactive phytocompounds from *Desmodium gangeticum* was retrieved from the IMPPAT database (https://cb.imsc.res.in/imppat/) and imported into Maestro version 12.8 for further analysis. The compounds were prepared for molecular docking using the LigPrep module, where they underwent energy minimization, protonation at physiological pH (7.0 ± 2.0), and generation of low-energy conformers (Ojo *et al.,* 2025). The LigPrep workflow was configured to desalt structures, generate possible tautomers and ionization states using Epik, and enumerate stereoisomers. All parameters in LigPrep, except those related to the generation of tautomers and stereoisomers (set to generate one stereoisomer per ligand), were maintained at default settings to ensure that the compounds were in their optimal conformational and ionization states for docking against the prepared MAO-B and 5-H2TA Proteins. The combination of these steps ensured that both the MAO-B and 5-HT2A structures and *Desmodium gangeticum* phytocompounds were fully optimized and ready for subsequent molecular docking analyses to predict potential binding interactions and affinities (Mohanraj *et al.,* 2022).

Molecular Docking

Docking was carried out using the Schrödinger suite's program Glide for estimating the interactions of the ligands with MAO-B and 5-H2TA one after the other, Glide uses a series of filters to search for the best-fit ligand conformations in the protein binding sites. Docking was performed in two steps: Standard Precision (SP) first to dock all compounds, and then Extra Precision (XP) mode for the top-scoring compounds. Glide XP aims to generate the best quality ligand poses by eliminating low energy poses and selecting the top-scoring ligands on the basis of energies and pose geometry. All the phytocompounds from IMPPAT and the standard drugs (Rasagiline; MAO-B, Ketanserin and Pimavanserin; 5-H2TA) were docked into the receptor grid. Post-docking minimization was allowed to optimize the binding poses. Glide sampled different ligand poses and scored them according to interaction energies, shape complementarity, and binding affinities, giving us the predicted binding poses for each of the compounds (Ramírez and Caballero, 2016).

ADME Prediction and Drug-Likeness Assessment

Pharmacokinetic and physicochemical property assessment via the Absorption, Distribution, Metabolism, and Excretion (ADME) profiling is a crucial step in drug discovery. These characteristics allow for the prediction of how the compounds will interact with the human physiological environment, especially in terms of absorption, distribution, metabolism, and excretion. After molecular docking, compounds from *Desmodium gangeticum* showing strong binding affinity with the chosen target were screened for ADME profiling using QikProp, an *in-silico* prediction program used for evaluating the potential pharmaceutical properties and pharmacokinetic parameters. Compounds with more than one violation of Lipinski's Rule of Five (Ro5) criteria were filtered out before the ADMET profiling. Next, the QikProp panel and ProTox-III toxicity prediction server were used to predict the absorption, distribution, metabolism, excretion, and toxicity (ADMET) (Banerjee *et al.,* 2024).

Binding Free Energy Calculation (MM-GBSA)

Further refinement of high docking score complexes was carried out using Prime MM-GBSA, which uses molecular mechanics and solvation models to estimate binding free energy (ΔGbind). Breakdown of the binding energy into van der Waals, electrostatic, hydrogen bonding, and solvation interactions allowed precise calculation of binding affinities (Genheden *et al.,* 2021).

Quantitative Structure-Activity Relationship (QSAR) Modeling

Quantitative Structure-Activity Relationship (QSAR) models were developed with AutoQSAR, an automated machine-learning tool for predictive modeling using structural or property data and biological activities. This software calculates molecular fingerprints and descriptors from 2D and 3D structures and uses regression or classification methods to establish relationships between molecular structures and properties.

An experimental dataset of MAO-B inhibitors and 5-H2TA modulators together with their IC50 values were obtained from the ChEMBL database (https://www.ebi.ac.uk/chembl/) by searching the MAO-B and 5-H2TA proteins' FASTA sequences, ensuring that the selected compounds were pertinent to the target proteins. The selected compounds were then cleaned in DataWarrior and prepared in LigPrep of Maestro to prepare the structures. IC50 values were transformed to pIC50 to make them linearly correlated with the descriptors. QSAR models were built using the structure and pIC50 values of the inhibitors with various algorithms such as k nearest neighbors (kNN), partial least squares (PLS), and random forest (RF). The model was chosen based on R^2, RMSE, and Q^2 values, and helps to understand the structure-activity relationship and lead optimisation ((Ojo *et al.,* 2025); Cherkasov *et al.,* 2024).

Molecular Dynamics (MD) Simulation

Molecular dynamics (MD) simulations were carried out only for MAO-B using the Schrödinger package to check the stability of the protein-ligand complexes as a function of time. The two phytochemicals (Desmodin and 5,7,2',4'-Tetrahydroxy-6-pre nylisoflavanone) with the best docking scores and MM-GBSA values, and rasagiline as a control, were simulated for 100 nanoseconds. Preparation of each protein-ligand complex was done using the Protein Preparation Wizard in Maestro, followed by system preparation using the System Builder. The complexes were solvated using the TIP3P water model in an orthorhombic box measuring 10×10×10 Å. Energy minimization and equilibration were performed under NPT ensemble conditions at 300 K and 1 bar using the OPLS4 force field. Trajectories were saved at 100 ps intervals for subsequent analysis. Stability was evaluated through root mean square deviation (RMSD) of protein and ligand over time. Additional analyses included protein RMSF, radius of gyration, intramolecular hydrogen bonds, protein-ligand interaction profiles, secondary structure elements, ligand RMSF, and solvent accessible surface area to characterize binding dynamics and complex stability (Ramírez and Caballero, 2016).

RESULT

Molecular docking

Molecular docking was performed to evaluate the binding potential of *D. gangeticum* phytochemicals against two therapeutic targets: MAO-B, implicated in Parkinson's motor symptoms, and the 5-HT2A receptor, associated with hallucinations and psychosis. The 2D binding interactions of selected compounds with MAO-B are shown in Figures 1–3, while those with the 5-HT2A receptor are presented in Figures 4–6. The molecular docking scores, interaction profiles, and predicted pIC_{50} values for MAO-B are summarized in Table 1, whereas those for the 5-HT2A receptor are presented in Table 2.

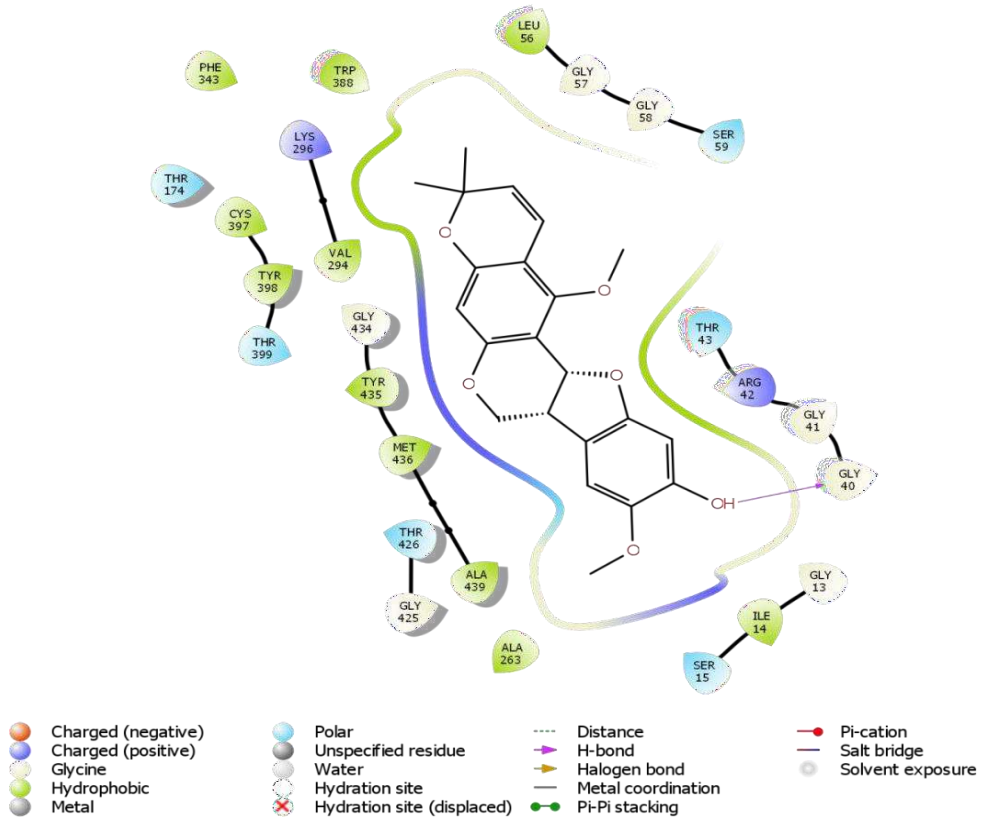


Figure **1:** 2D Interaction of desmodin with amino acid residue within MAO-B binding site, demonstrating how the compound interacts at the atomic level.

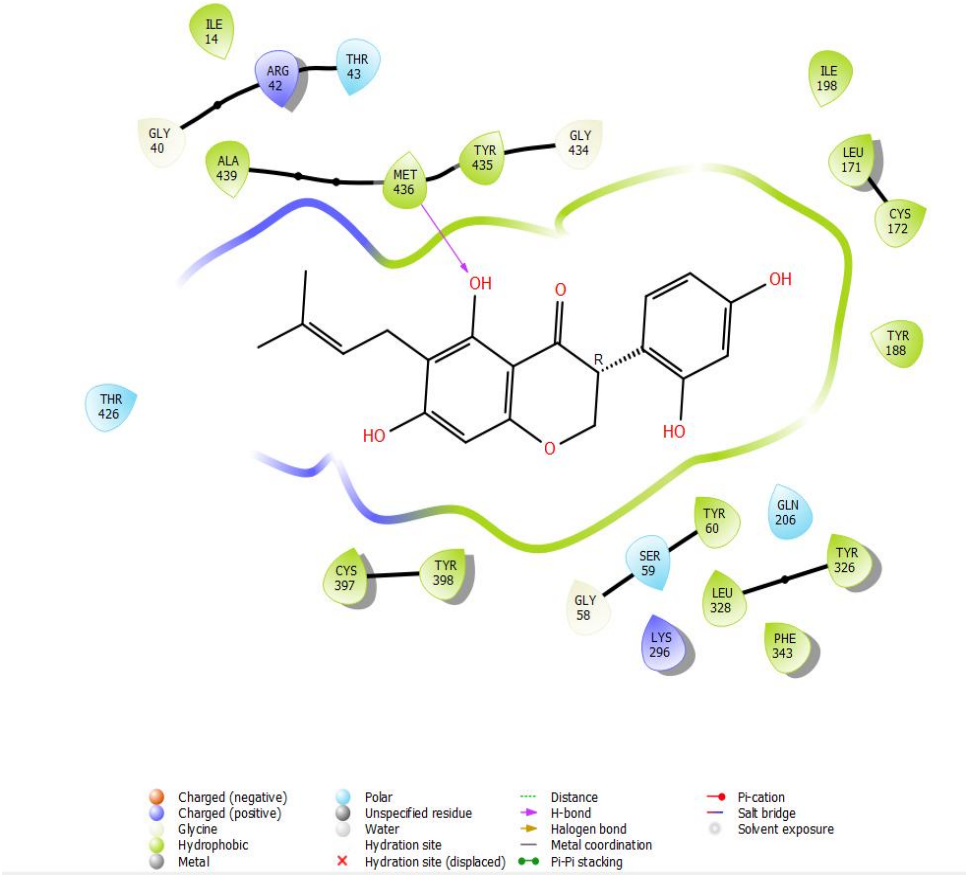


Figure **2***:* 2D Interaction of 5,7,2',4'-Tetrahydroxy-6-prenylisoflavanone with amino acid residue within MAO-B binding site, demonstrating how the compound interacts at the atomic level

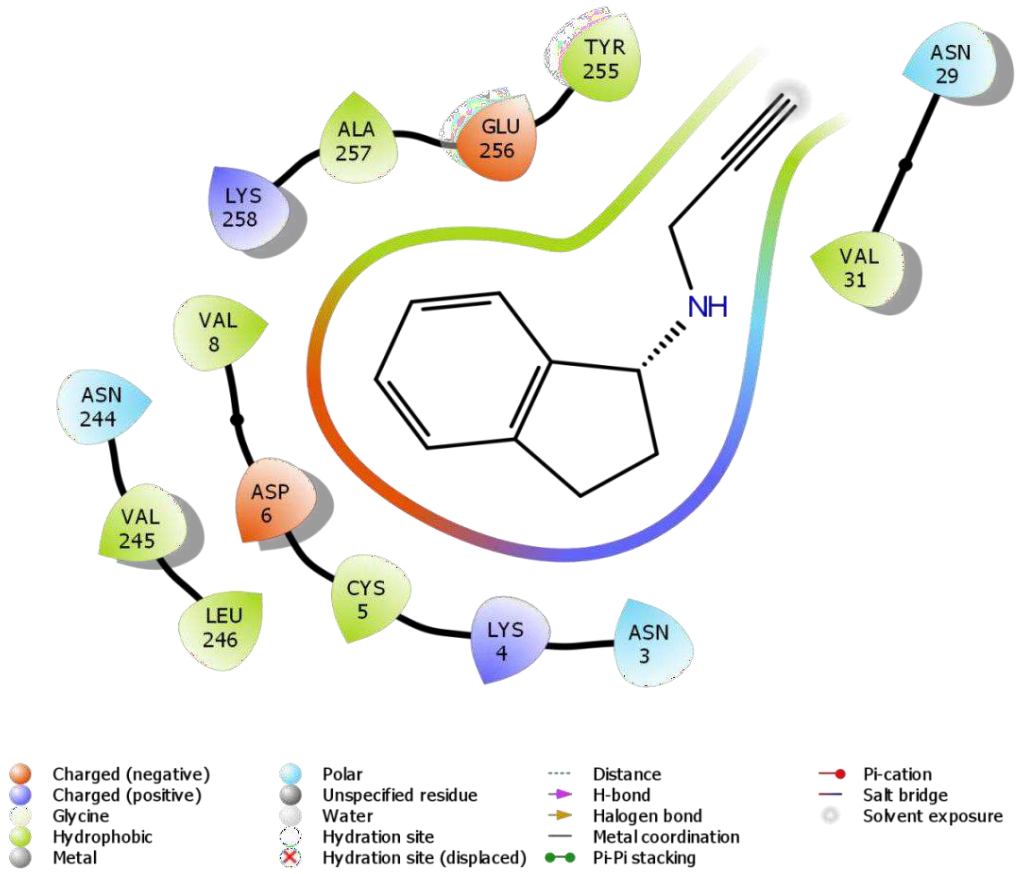


Figure **3:** 2D Interaction of rasagiline with amino acid residue within MAO-B binding site, demonstrating how the compound interacts at the atomic level

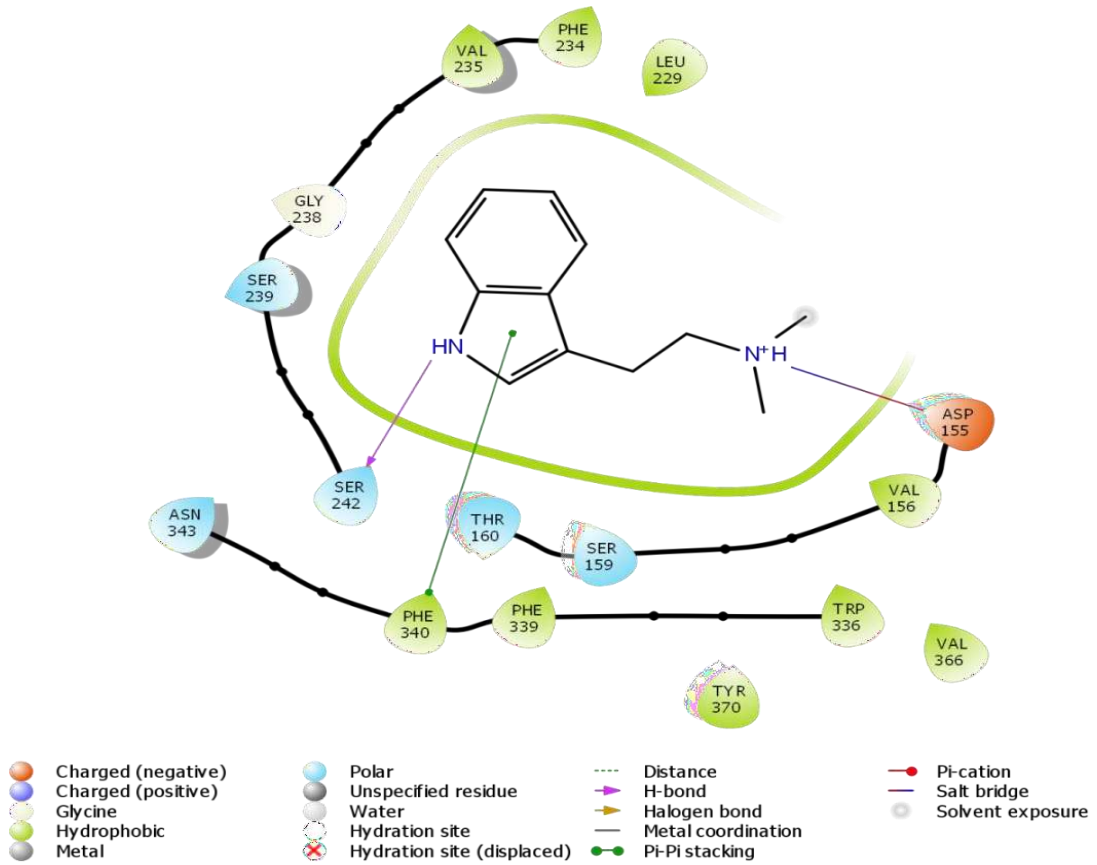


Figure **4:** 2D Interaction of N, N-Dimethyltryptamine with amino acid residue within 5HT2A binding site, demonstrating how the compound interacts at the atomic level

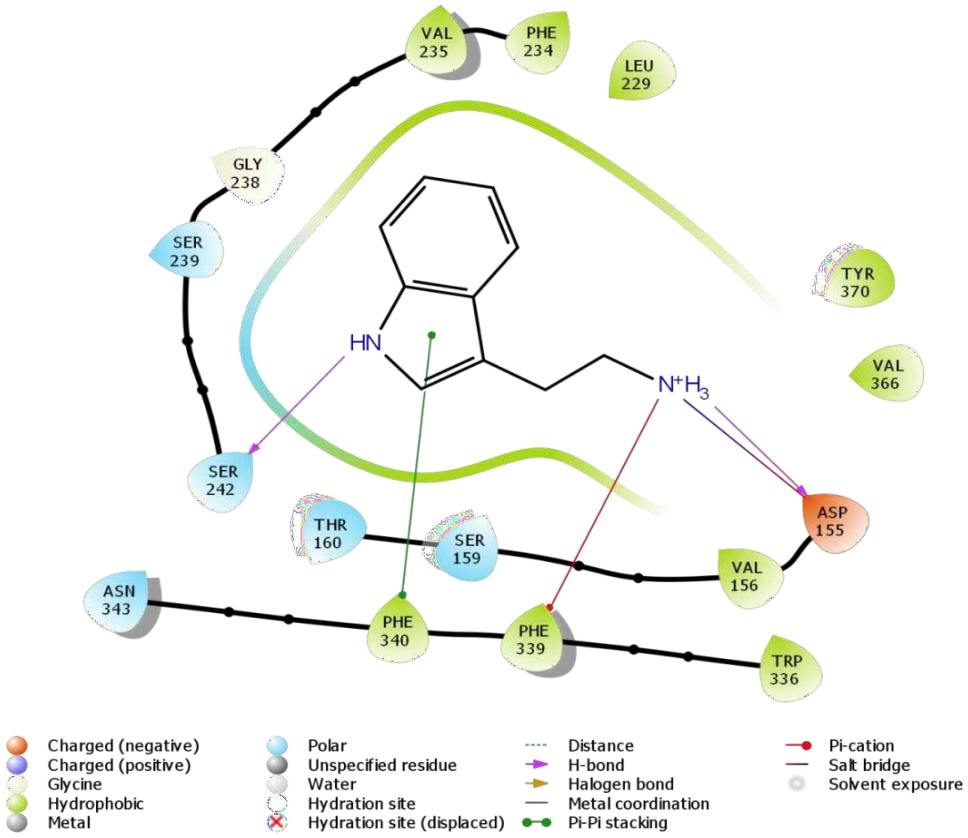


Figure **5:** 2D Interaction of tryptamine with amino acid residue within 5HT2A binding site, demonstrating how the compound interacts at the atomic level

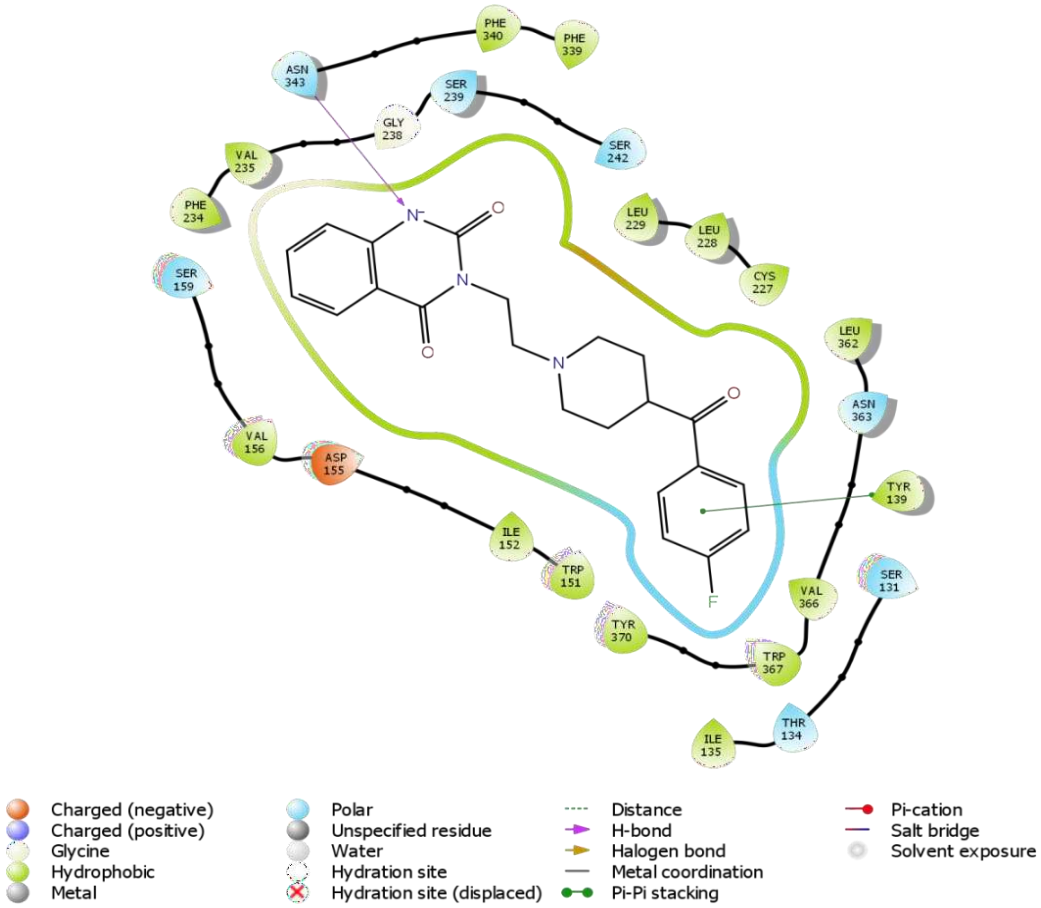


Figure **6:** 2D Interaction of ketanserin - 5HT2A with amino acid residue within 5HT2A binding site, demonstrating how the compound interacts at the atomic level

Table **1:** Molecular docking results of *Desmodium gangeticum* lead phytochemicals against MAO-B with rasagiline as the reference inhibitor.

S/n	Ligand Name	Hydrophobic interaction	Hydrogen bond interaction	Docking score	pIC50
1	Desmodin	ILE14, ALA263, ALA439, MET436, TYR435, TYR398, CYS397, VAL294, PHE60, TRP388, LEU56	GLY 40	-9.901	4.775
2	5,7,2',4'-Tetrahydroxy-6-prenylisoflavanone.	ILE14, ALA439, MET436, CYS397, TYR398, TYR60, TYR326, PHE384, LEU328, TYR188, LEU171, CYS172, ILE198	MET436	-8.933	4.699
3	Kievitone	ILE, ALA439, MET436, TYR435, TYR398, CYS397, PHE343, VAL294, TYR60, TRP388, LEU56	TYR60, GLY434	-8.60	4.352
4	Dalbergiodin	TYR398, TYR435, MET436, ILE198, ILE199, CYS172, LEU171, PHE343, TYR326, LEU328, GLY205, GLN206, TYR60, SER59, GLY58	GLN206, SER59	-7.846	4.303
5	2`-Hydroxygenistein	ARG36, ALA35, GLU34, LEU268, PRO265, ILE264, ALA263, GLY11, GLY12, GLY13, ILE14, SER15, GLY16, THR426, TYR393, SER394, GLY41, ARG42, ALA439	GLY16, GLU34, ALA263	-6.780	4.946
6	Rasagiline (SD)	LEU246, VAL245, CYS5, VAL8, ALA257, TYR255, VAL31		-5.808	4.717

Table **2:** Molecular docking profiles of *Desmodium gangeticum* lead phytochemicals against the 5-HT2A receptor, with ketanserin and pimavanserin as reference inhibitors.

S/n	Ligand Name	Hydrophobic interaction	Hydrogen bond interaction	Docking score	pIC50
1	N, N-Dimethyltryptamine	TYR370, VAL366, TRP336, PHE339, PHE340, VAL156, VAL235, PHE234, LEU229	SER242	-8.648	6.234
2	Tryptamine	TRP336, PHE339, PHE340, VAL156, VAL235, PHE234, LEU229, TYR370, VAL366	ASP155, SER242	-8.647	6.234
3	N, N-Dimethyl-5-methoxyTryptamine	TRP336, PHE339, PHE340, VAL235, PHE234, LEU229, ILE152, VAL366, AL156, TYR370	SER242	-8.134	6.002
4	Desmodin	PHE234, VAL235, TYR370, TRP336, PHE339, PHE340, VAL156, ILE210, ILE152, TRP151, LEU229, LEU228, CYS227, TYR139, LEU362	ASN363	-7.900	5.742
5	Nb-methyltetrahydroharman	TRP336, PHE339, PHE340, ILE152, VAL156, LEU229, VAL235, PHE234, VAL366, TYR370	ASP155	-7.822	6.234
6	Ketanserin (SD)	ILE135, TYR370, TRP367, VAL366, TYR362, CYS227, LEU228, LEU229, VAL235, PHE234, VAL156, ILE152, TRP151, PHE340, PHE339	ASN343	-5.085	6.234
7	Pimavanserin (SD)	PHE339, PHE340, TRP151, ILE152, VAL156, PHE234, VAL235, ILE210, TYR139, TRP141, LEU362, VAL366, CYS227, LEU228, LEU229	LEU229	-4.918	5.939

ADMET Profiling

ADMET profiling was carried out to assess the pharmacokinetics and drug-likeness of the lead phytochemicals. The properties evaluated were molecular weight (mol_MW), hydrogen bond donors (DonorHB), hydrogen bond acceptors (AccptHB), lipophilicity (QPlogPo/w), polar surface area (PSA), human serum album binding (QPlogKhsa), blood-brain barrier penetration (QPlogBB), and Lipinski's Rule of Five. The ADMET properties of compounds targeting MAO-B and 5-HT2A are presented in Tables 3 and 4, respectively.

Table **3:** ADMET profiles of *Desmodium gangeticum* lead phytochemicals targeting MAO-B.

S/n	Ligand Name	mol_MW	Donor Hb	Accpt HB	QPlogPo/w	PSA	QPlogBB	QPlog Khsa	RuleOfFive
1	Desmodin	382.412	1	5	4.281	62.235	-0.121	0.685	0
2	5,7,2',4'-Tetrahydroxy-6-prenylisoflavanone	356.374	3	5	2.584	113.618	-1.758	0.279	0
3	Kievitone	356.374	3	5	2.702	111.482	-1.744	0.315	0
4	Dalbergiodin	288.256	3	5	1.006	119.0	-1.624	0.210	0
5	2`-Hydroxygenistein	240.240	3	5	1.052	120.9	-1.741	0.254	0
6	Rasagiline (SD)	171.241	2	2	2.374	13.001	0.649	-0.026	0

Table **4:** ADMET profiles of *Desmodium gangeticum* lead phytochemicals targeting 5-HT2A.

S/n	Ligand Name	mol_MW	Donor HB	Accpt HB	QPlog Po/w	PSA	QPlog Khsa	QPlog BB	Ruleof5
1	N, N-DimethylTryptamine	188.272	1	2	2.498	19.510	0.097	0.489	0
2	Tryptamine	160.218	3	1	1.182	41.118	-0.362	0.030	0
3	N, N-Dimethyl-5-methoxyTryptamine	218.298	1	2	2.620	27.244	0.114	0.459	0
4	Desmodin	382.412	1	4	4.395	60.135	0.727	-0.131	0
5	Nb-methyltetrahydroharman.	200.283	1	2	2.546	18.424	0.227	0.781	0
6	Ketanserin (SD)	395.432	1	7	2.800	96.675	0.241	-0.806	0
7	Pimavanserin (SD)	427.561	1	4	4.779	41.462	0.706	0.329	0

Toxicology Profiling

The lead phytochemicals were assessed for toxicity *in silico*. The evaluation criteria included hepatotoxicity, carcinogenicity, mutagenicity, cytotoxicity, and predicted median lethal dose (LD_{50}). The toxicological profiles of the prioritized compounds against MAO-B and the 5-HT2A receptor are presented in Tables 5 and 6, respectively.

Table **5:** Predicted toxicological profiles of *Desmodium gangeticum* lead phytochemicals targeting MAO-B, with rasagiline as the reference inhibitor.

S/n	Ligand Name	Hepatotoxicity	Carcinogenicity	Mutagenicity	Cytotoxicity	Predicted LD50
1	Desmodin	Inactive	Inactive	Inactive	Inactive	500mg/kg
2	5,7,2',4'-Tetrahydroxy-6-prenylisoflavanone	Inactive	Inactive	Inactive	Inactive	890mg/kg
3	Kievitone	Inactive	Inactive	Inactive	Inactive	10mg/kg
4	Dalbergiodin	Inactive	Inactive	Inactive	Inactive	2647mg/kg
5	2`-Hydroxygenistein	Inactive	Inactive	Inactive	Inactive	600mg/kg
6	Rasagiline	Inactive	Inactive	Inactive	Inactive	250mg/kg

Table **6:** Predicted toxicological profiles of *Desmodium gangeticum* lead phytochemicals targeting 5-HT2A, with ketanserin and pimavanserin as reference inhibitors.

S/n	Ligand Name	Hepatotoxicity	Carcinogenicity	Mutagenicity	Cytotoxicity	predicted LD50
1	N, N-DimethylTryptamine	Inactive	Inactive	Inactive	Inactive	225mg/kg
2	Tryptamine	Inactive	Inactive	Inactive	Inactive	940mg/kg
3	N, N-Dimethyl-5-methoxyTryptamine	Inactive	Inactive	Inactive	Inactive	963mg/kg
4	Desmodin	Inactive	Inactive	Inactive	Inactive	500mg/kg
5	Nb-methyltetrahydroharman.	Inactive	Inactive	Inactive	Inactive	500mg/kg
6	Ketanserin (SD)	Inactive	Inactive	Inactive	Inactive	790mg/kg
7	Pimavanserin (SD)	Inactive	Inactive	Inactive	Inactive	3000mg/kg

MM-GBSA Binding Free Energy

To assess the stability and thermodynamics of the protein–ligand complexes, MM-GBSA binding free energy calculations were performed. The parameters evaluated included the overall binding free energy (ΔG Bind), covalent, hydrogen bond, solvation (ΔG Bind Solv GB), and van der Waals energy (ΔG Bind vdW). The MM-GBSA results for the lead compounds against MAO-B and the 5-HT2A receptor are presented in Tables 7 and 8, respectively.

Table **7:** MM-GBSA binding free energy components of *Desmodium gangeticum* lead phytochemicals with MAO-B.

S/n	Ligand Name	MMGBSA dG Bind (kcal/mol)	MMGBSA dG Bind Covalent (kcal/mol)	MMGBSA dG Bind Hbond (kcal/mol)	MMGBSA dG Bind Solv GB (kcal/mol)	MMG BSA dG Bind vdW (kcal/mol)
1	Desmodin	-40.42	20.69	-1.42	36.13	-31.17
2	5,7,2',4'-Tetrahydroxy-6-prenylisoflavanone	-30.88	6.08	-1.14	45.88	-54.89
3	Kievitone	-56.18	9.33	-1.64	27.42	-46.17
4	Dalbergioidin	-40.31	1.19	-1.49	35.80	-40.93
5	2`-Hydroxygenistein	-40.23	3.78	-3.97	23.08	-40.84
6	Rasagiline (SD	-42.32	3.03	-1.14	7.44	-29.88

Table **8:** MM-GBSA binding free energy components of *Desmodium gangeticum* lead phytochemicals with 5-HT2A.

S/n	Ligand Name	MMGBSA dGBind (kcal/mol)	MMGBSA dGBind Covalent (kcal/mol)	MMGBSA dGBind Hbond (kcal/mol)	MMGBSA dGBind Solv GB (kcal/mol)	MMGBSA dGBind vdW (kcal/mol)
1	N, N-DimethylTryptamine	-44.7	1.94	-1.73	41.14	-27.27
2	Tryptamine	-43.53	0.4	-1.39	42.07	-28.11
3	N, N-Dimethyl-5-methoxyTryptamine	-42.87	5.68	-1.83	43.2	-24.6
4	Desmodin	-51.69	8.63	-1.37	26.15	-37.72
5	Nb-methyltetrahydroharman	-38.5	2.9	-1.02	37.25	-25.2
6	Ketanserin (SD)	-27.55	10.85	-0.64	29.82	-53.09
7	Pimavanserin (SD)	4.08	15.13	-0.61	47.37	4.71

QSAR Modeling

QSAR modeling was used to validate the docking results and estimate the activities of the lead phytochemicals. AutoQSAR analysis produced predictive models for each protein target, and compound activities were compared with experimentally observed values. The statistical parameters of the best-performing models for MAO-B and the 5-HT2A receptor are presented in Tables 9 and 11, respectively, while the corresponding predicted and observed activities of the compounds are shown in Tables 10 and 12.

Table **9:** Parameters corresponding to the best predictive model generated by AutoQSAR for MAO-B activity prediction.

Model code	Score	SD	R 2	RMSE	Q 2
kpls_linear_49	0.760125	0.5774	0.8404	0.6042	0.7567

Table **10:** AutoQSAR-predicted activities of *Desmodium gangeticum* lead phytochemicals compared with observed values for MAO-B inhibition.

S/n	Set	pIC50 (observed)	pIC50 (predicted)	Residue error	ChEMBL ID
1	train	4.08	4.0298	-0.0502	CHEMBL3408925
2	train	4.02	3.9018	-0.1182	CHEMBL3408927
3	train	5	5.6526	0.6526	CHEMBL472716
4	test	5.94	4.9276	-1.0124	CHEMBL515237
5	test	8	7.626	-0.374	CHEMBL375966
6	train	7.52	7.7953	0.2753	CHEMBL385397
7	train	4.6	4.8093	0.2093	CHEMBL489084
8	train	6.07	5.1502	-0.9198	CHEMBL489085
9	train	9	8.822	-0.178	CHEMBL424940
10	train	5.22	6.1999	0.9799	CHEMBL218323
11	test	6.7	5.9627	-0.7373	CHEMBL474940
12	train	6	6.4346	0.4346	CHEMBL972
13	test	6.35	6.9875	0.6375	CHEMBL221593
14	train	5.35	5.4942	0.1442	CHEMBL472903
15	train	5.95	5.3282	-0.6218	CHEMBL472904
16	train	4	4.3198	0.3198	CHEMBL473309
17	train	5.87	5.7058	-0.1642	CHEMBL474939
18	train	5	4.8921	-0.1079	CHEMBL447022
19	test	4	4.8358	0.8358	CHEMBL515250
20	train	4	3.9187	-0.0813	CHEMBL472713
21	test	4.82	4.8047	-0.0153	CHEMBL18116
22	test	5.79	5.1616	-0.6284	CHEMBL514151
23	train	7	6.8696	-0.1304	CHEMBL375616
24	train	4	4.7195	0.7195	CHEMBL221629
25	train	8.22	8.4195	0.1995	CHEMBL218059
26	train	4.01	4.1462	0.1362	CHEMBL8706
27	train	4.21	4.2762	0.0662	CHEMBL3585818
28	train	4.08	3.7509	-0.3291	CHEMBL3585822
29	train	4.09	3.8017	-0.2883	CHEMBL3408922
30	train	6.82	5.8695	-0.9505	CHEMBL472918
31	test	4	5.0752	1.0752	CHEMBL514297
32	train	5.89	5.9403	0.0503	CHEMBL515389
33	train	5.79	5.7133	-0.0767	CHEMBL474738
34	test	4.7	4.9461	0.2461	CHEMBL50
35	train	6.82	5.9284	-0.8916	CHEMBL472902
36	train	4	4.9579	0.9579	CHEMBL508175
37	train	8.05	7.5481	-0.5019	CHEMBL221293
38	train	7.39	6.0716	-1.3184	CHEMBL218324
39	train	4	4.9496	0.9496	CHEMBL505492
40	train	5	4.9594	-0.0406	CHEMBL489086
41	train	6	6.4346	0.4346	CHEMBL972
42	test	5	5.0843	0.0843	CHEMBL514139
43	train	4.58	4.238	-0.342	CHEMBL3408924

44	train	4	4.4411	0.4411	CHEMBL472712
45	train	4.82	4.8047	-0.0153	CHEMBL18116
46	test	4.11	4.6108	0.5008	CHEMBL3415439
47	test	4.07	3.8614	-0.2086	CHEMBL3585817
48	test	4.01	4.1462	0.1362	CHEMBL8706
49	train	4.06	4.1997	0.1397	CHEMBL3408928
50	train	4.06	4.1975	0.1375	CHEMBL3585814
51	train	5.62	4.6452	-0.9748	CHEMBL523765
52	train	5.2	6.053	0.853	CHEMBL508959

Table **11:** Parameters corresponding to the best predictive model generated by AutoQSAR for 5-HT2A activity prediction.

Model code	**Score**	**SD**	**R 2**	**RMSE**	**Q 2**
kpls_linear_5	0.760125	0.3574	0.8916	0.2997	0.9046

Table **12:** AutoQSAR-predicted activities of *Desmodium gangeticum* lead phytochemicals compared with observed values for 5-HT2A modulation.

S/n	**Set**	**pIC50 (observed)**	**pIC50 (predicted)**	**Residue error**	**ChEMBL ID**
1	test	5.0000	5.0662	0.0662	CHEMBL4635729
2	train	6.0000	6.0249	0.0249	CHEMBL4635373
3	train	5.0000	5.0216	0.0216	CHEMBL2206440
4	train	5.0000	4.8311	-0.1689	CHEMBL4646835
5	train	5.0000	5.1742	0.1742	CHEMBL4645305
6	test	6.1800	6.0249	-0.1551	CHEMBL4645193
7	train	6.1600	6.0249	-0.1351	CHEMBL4635960
8	train	7.6200	7.9759	0.3559	CHEMBL4638006
9	train	6.0000	6.0249	0.0249	CHEMBL4639821
10	test	6.1600	6.0249	-0.1351	CHEMBL4635960
11	train	5.0000	5.7781	0.7781	CHEMBL4642761
12	test	6.1000	6.0249	-0.0751	CHEMBL4639821
13	test	5.0000	5.0216	0.0216	CHEMBL2206440
14	train	6.8600	6.0249	-0.8351	CHEMBL4641860
15	train	5.0000	4.6546	-0.3454	CHEMBL4643961
16	train	6.2900	6.0249	-0.2651	CHEMBL4638687
17	train	5.9300	6.0249	0.0949	CHEMBL4641860
18	test	6.8500	6.0249	-0.8251	CHEMBL4641860
19	train	6.0000	6.0249	0.0249	CHEMBL4639821
20	train	7.6200	7.9759	0.3559	CHEMBL4638006
21	train	7.5400	7.6949	0.1549	CHEMBL4636980
22	test	5.7200	6.0249	0.3049	CHEMBL4635373

23	train	6.1800	6.0249	-0.1551	CHEMBL4645193
24	train	6.3300	6.0249	-0.3051	CHEMBL4645193
25	train	7.6400	7.6949	0.0549	CHEMBL4636980
26	test	7.6600	7.8596	0.1996	CHEMBL489624
27	train	6.3800	6.0249	-0.3551	CHEMBL4638687
28	train	6.4200	6.0249	-0.3951	CHEMBL4635960
29	train	5.7200	6.0249	0.3049	CHEMBL4635373
30	train	5.9200	6.0249	0.1049	CHEMBL4641860
31	test	7.6400	7.6949	0.0549	CHEMBL4636980
32	train	8.2600	7.9759	-0.2841	CHEMBL4638006
33	train	6.0900	6.0249	-0.0651	CHEMBL4639821
34	test	6.4200	6.0249	-0.3951	CHEMBL4635960
35	train	5.0000	5.1742	0.1742	CHEMBL4645305
36	train	5.0000	4.9640	-0.0360	CHEMBL4632373
37	test	5.0000	5.0662	0.0662	CHEMBL4635729
38	train	6.5100	6.0249	-0.4851	CHEMBL4641860
39	train	5.2800	5.7781	0.4981	CHEMBL4642761
40	test	6.0500	6.0249	-0.0251	CHEMBL4638687
41	train	5.0100	5.7781	0.7681	CHEMBL4642761
42	train	5.6200	6.0249	0.4049	CHEMBL4635373
43	train	8.2100	7.9759	-0.2341	CHEMBL4638006
44	train	7.8000	7.6949	-0.1051	CHEMBL4636980
45	train	5.0000	4.8311	-0.1689	CHEMBL4646835
46	train	8.0400	7.8596	-0.1804	CHEMBL489624
47	train	5.1000	5.7781	0.6781	CHEMBL4642761
48	train	5.8000	6.0249	0.2249	CHEMBL4635960
49	test	7.5400	7.6949	0.1549	CHEMBL4636980
50	train	5.8000	6.0249	0.2249	CHEMBL4635960
51	train	7.6400	7.8596	0.2196	CHEMBL489624
52	test	5.2800	5.7781	0.4981	CHEMBL4642761
53	train	6.0500	6.0249	-0.0251	CHEMBL4638687
54	train	7.6600	7.8596	0.1996	CHEMBL489624
55	train	5.6200	6.0249	0.4049	CHEMBL4635373
56	test	6.3700	6.0249	-0.3451	CHEMBL4638687
57	train	6.3200	6.0249	-0.2951	CHEMBL4645193
58	test	8.0400	7.8596	-0.1804	CHEMBL489624
59	train	5.1000	5.7781	0.6781	CHEMBL4642761
60	train	5.7700	6.0249	0.2549	CHEMBL4639821
61	train	6.5700	6.0249	-0.5451	CHEMBL4645193
62	train	6.2900	6.0249	-0.2651	CHEMBL4638687
63	train	6.5200	6.0249	-0.4951	CHEMBL4641860
64	test	5.8100	6.0249	0.2149	CHEMBL4639821
65	train	6.5700	6.0249	-0.5451	CHEMBL4645193

66	train	7.6400	7.8596	0.2196	CHEMBL489624
67	train	8.2700	7.9759	-0.2941	CHEMBL4638006
68	train	5.0000	4.9640	-0.0360	CHEMBL4632373
69	train	8.2100	7.9759	-0.2341	CHEMBL4638006
70	train	7.7900	7.6949	-0.0951	CHEMBL4636980
71	test	5.0000	4.6546	-0.3454	CHEMBL4643961
72	test	5.9800	6.0249	0.0449	CHEMBL4635373

Molecular Dynamics Simulation

Molecular dynamics simulations were performed to evaluate the stability of the MAO-B complexes over a 100 ns trajectory. The structural dynamics of Desmodin, 5,7,2′,4′-tetrahydroxy-6-prenylisoflavanone, and rasagiline complexes are presented in Figures 7–11. Key parameters including root mean square deviation (RMSD), root mean square fluctuation (RMSF), radius of gyration (Rg), solvent accessible surface area (SASA), hydrogen bond stability, and Ramachandran analysis were used to assess system stability.

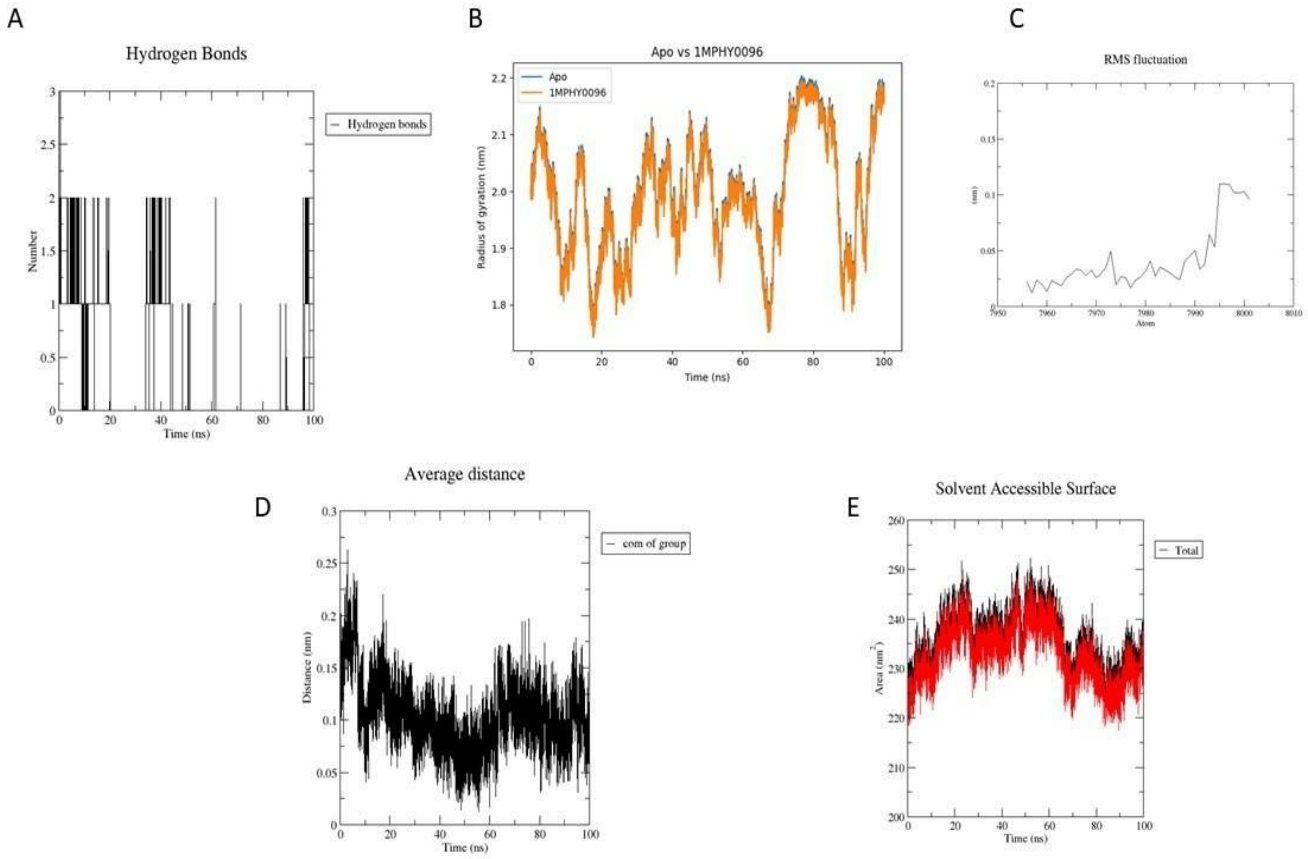


Figure **7:** Molecular dynamics simulation of the Desmodin–MAO-B complex and apo MAO-B over a 100 ns trajectory.

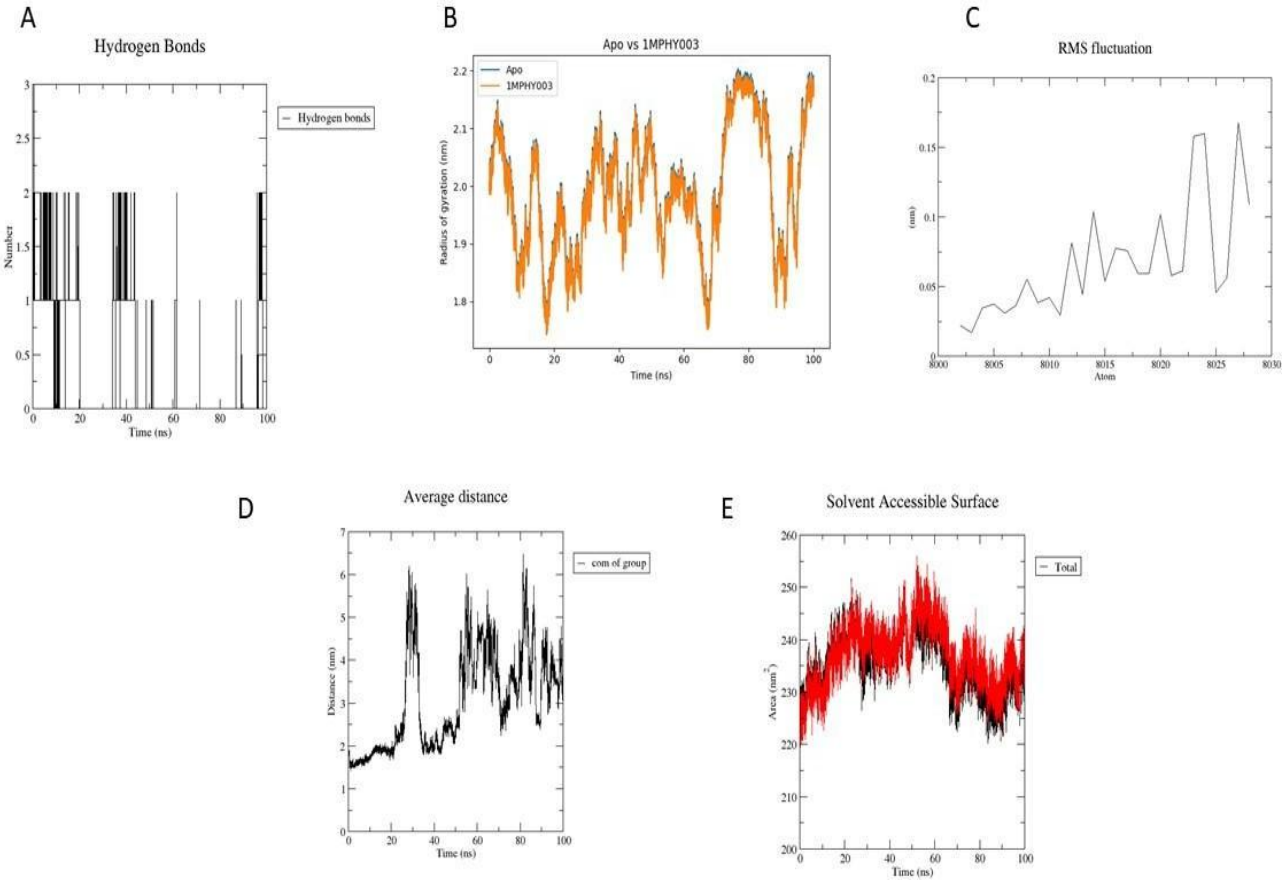


Figure **8:** Molecular dynamics simulation of the 5,7,2′,4′-tetrahydroxy-6-prenylisoflavanone–MAO-B complex and apo MAO-B over a 100ns trajectory.

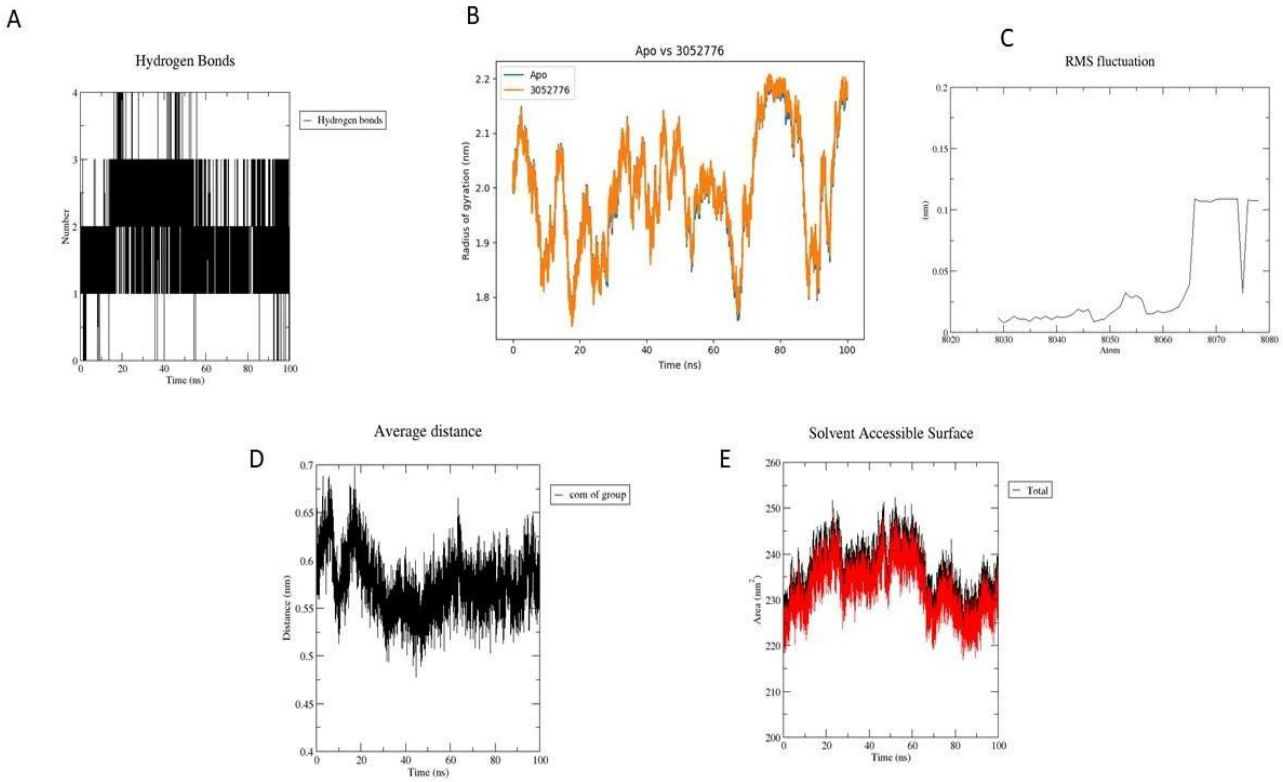


Figure **9:** Molecular dynamics simulation of the Rasagiline–MAO-B complex and apo MAO-B over a 100ns trajectory.

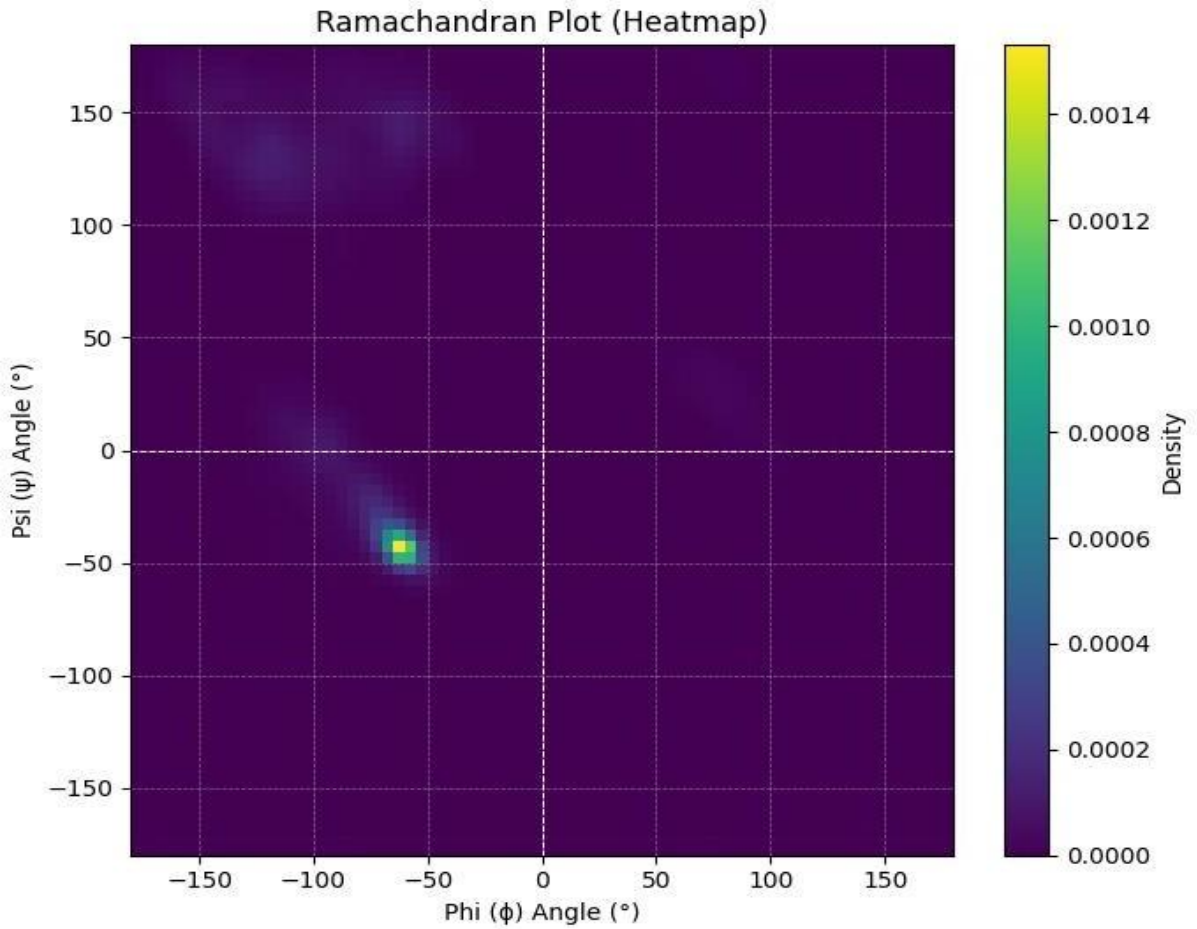


Figure **10:** Ramachandran plot showing backbone dihedral angle distributions across the simulated MAO-B complexes.

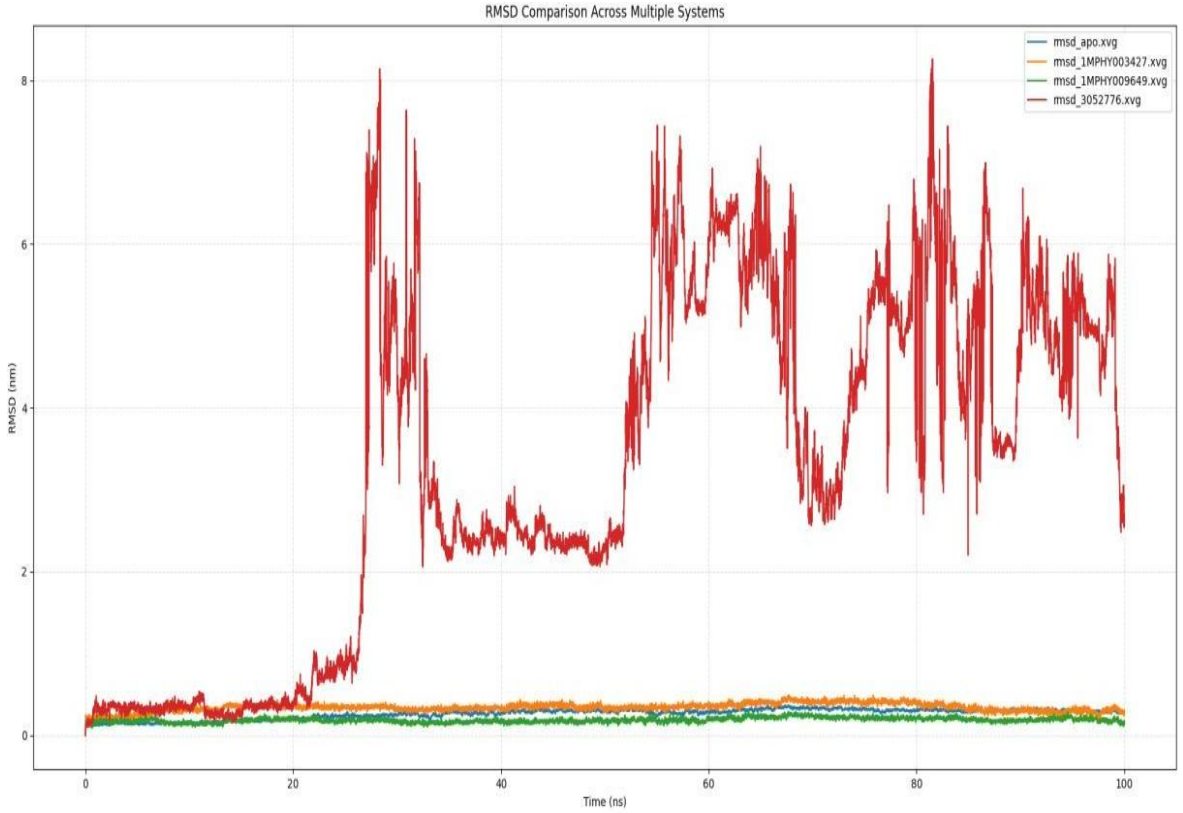


Figure **11:** RMSD comparison of MAO-B apo-protein and complexes with Desmodin, 5,7,2′,4′-Tetrahydroxy-6-prenylisoflavanone, and the reference inhibitor Rasagiline over a 100 ns trajectory.

DISCUSSION

This study offers a comprehensive in-silico profiling of the *Desmodium gangeticum* phytochemicals as dual regulators of monoamine oxidase-B (MAO-B) and 5-hydroxytryptamine type 2A (5-HT2A), two mechanistic but clinically overlapping targets in Parkinson's disease. The motor dysfunction seen in PD is caused by a loss of dopamine, which is corrected by MAO-B inhibition (Singh *et al.,* 2024), but dopaminergic treatments also worsen neuropsychiatric side effects such as hallucinations and delusions. These hallucinations are intimately associated with serotonin signaling abnormalities, particularly hyperactivation of 5-HT2A receptors (Kwan *et al.,* 2021). Accordingly, PD pathology is characterised by a dopamine/serotonin imbalance, where efforts to alleviate motor symptoms also exacerbate non-motor symptoms (Kwan *et al.,* 2021).

Our research notes that *D. gangeticum* phytochemicals have structural similarities that allow them to modulate both: maintaining normal dopamine levels by inhibiting MAO-B enzymes, and blocking serotonin-induced hallucinations via 5-HT2A antagonism (Rani *et al.,* 2022). This multi-targeting approach aims to solve the therapeutic conundrum in PD treatment, where dopaminergic therapies relieve motor symptoms but exacerbate psychosis, while antipsychotics treat psychosis but exacerbate motor dysfunction (Pirker, 2026). Through the combination of good docking scores, free binding energies, pharmacokinetic stability, and predicted safety margins for both targets, this study suggests that metabolites of *D. gangeticum* have the potential to achieve dual modulation of motor and non-motor aspects of PD.

Analysis of molecular docking was performed as the initial step, with ligand–receptor interactions illustrated in Figure 1–6. Desmodin showed the highest affinity for MAO-B (Table 1) with a docking score of -9.901 and predicted pIC_{50} of 4.775 (compared to reference inhibitor rasagiline's -5.808, pIC_{50} = 4.717). Hydrophobic interactions with ILE14, ALA263, ALA439, MET436, TYR435, TYR398, CYS397, VAL294, PHE60, TRP388, and LEU56 as well as a hydrogen bond with GLY40, also contributed to its stability. 5,7,2′,4′-Tetrahydroxy-6-prenylisoflavanone followed closely with a docking score of -8.933 and pIC_{50} of 4.699, engaging residues ILE14, ALA439, MET436, CYS397, TYR398, TYR60, TYR326, PHE384, LEU328, TYR188, LEU171, CYS172, and ILE198, with a hydrogen bond to MET436. Other plant compounds, including Kievitone, Dalbergioidin and 2`-Hydroxygenistein, exhibited strong binding, with 2`-Hydroxygenistein, being particularly interesting for its enhanced pIC_{50}. For 5-HT2A (Table 2), N, N-Dimethyltryptamine and Tryptamine scored -8.648 and pIC_{50} 6.234, interacting with TYR370, VAL156, VAL235, VAL366, TRP336, PHE234, PHE339, PHE340, and LEU229, with hydrogen bonding to SER242 and ASP155. Desmodin also exhibited good binding (-7.900, pIC_{50} 5.742), highlighting its dual-target capabilities. Overall, the docking results highlight Desmodin and 5, 7, 2′, 4′-tetrahydroxy-6-prenylisoflavanone as potential MAO-B inhibitors, and N, N-dimethyltryptamine and Tryptamine as the best 5-HT2A regulators. This finding is consistent with earlier reports that have demonstrated binding affinity of plant chemicals towards MAO-B similar to those of standard inhibitors, and that the stability of the binding should be attributed to the interactions with the key hydrophobic and hydrogen bond residues (Merghany *et al.,* 2025; Ajala *et al.,* 2024).

ADMET and drug-likeness analysis affirmed pharmacokinetic potential against standard drugs for the CNS. For MAO-B (Table 3), Desmodin and 5,7,2′,4′-Tetrahydroxy-6-prenylisoflavanone and the other plant compounds adhered to Lipinski's Rule of Five (Shruti and Bharadvaja, 2024) and had favourable physicochemical properties for blood-brain barrier (BBB) penetration. In the case of 5-HT2A (Table 4), N, N-Dimethyltryptamine and Tryptamine exhibited better BBB penetration and better physicochemical properties than ketanserin and pimavanserin, with restricted PSA and QPlogBB. Desmodin also showed adequate ADMET properties for 5-HT2A, confirming its potential as a dual-target modulator. Conclusively, the findings are in line with recent developments in computational toxicology and drug design for CNS diseases, which highlight physicochemical factors for BBB crossing and toxicity (Lee *et al.,* 2025; Alves *et al.,* 2025).

The ADMET profile was reinforced by toxicological predictions. MAO-B inhibitors (Table 5) were predicted to be non-toxic for hepatotoxicity, carcinogenicity, mutagenicity, and cytotoxicity. LD_{50} values spanned from 10 mg/kg for Kievitone to 890 mg/kg for 5,7,2′,4′-Tetrahydroxy-6-prenylisoflavanone, with Desmodin and 2`-Hydroxygenistein falling in the intermediate

range of 250-600 mg/kg and Dalbergiodin having the highest LD_{50} value 2647mg/kg. Rasagiline had 250 mg/kg, fitting into this toxicity range. For 5-HT2A modulators (Table 6), LD_{50} values spanned from 225 mg/kg for N, N-Dimethyltryptamine to 963 mg/kg for N, N-Dimethyl-5-methoxytryptamine, with Tryptamine at 940 mg/kg, and Desmodin and Nb-methyltetrahydroharman at 500 mg/kg. Ketanserin was found to be 790 mg/kg and pimavanserin 3000 mg/kg, the latter signifying very low acute toxicity. The two sets of phytochemicals were predicted to be completely inactive for hepatotoxicity, carcinogenicity, mutagenicity, and cytotoxicity, thereby suggesting acceptable safety profiles compared to the reference drugs. Together, these estimates of toxicity align with current research in computational toxicology and artificial intelligence (AI)-based ADMET (absorption, distribution, metabolism, excretion, and toxicity) models that focus on early assessment of liver toxicity, carcinogenicity, mutagenicity, and acute toxicity in the drug discovery process (Zhang *et al.,* 2025; Lee *et al.,* 2025).

MM-GBSA free energy calculations offered further insights into ligand - protein stability. In MAO-B (Table 7), Desmodin (ΔG Bind -40.42 kcal/mol; van der Waals -31.17 kcal/mol) and 5,7,2′,4′-Tetrahydroxy-6-prenylisoflavanone (-30.88 kcal/mol; van der Waals -54.89 kcal/mol) were the top picks with strong hydrophobic interactions, while Dalbergiodin and 2`-Hydroxygenistein also demonstrated strong bindings (-40.93 and -40.84 kcal/mol). For 5-HT2A (Table 8), Desmodin (-51.69 kcal/mol; van der Waals -37.72 kcal/mol) and N, N-Dimethyltryptamine (-44.70 kcal/mol; van der Waals -27.27 kcal/mol) emerged as the most intriguing, with their binding energy supported by balanced hydrophobic and hydrogen bonding interactions, while Tryptamine also demonstrated strong binding (-43.53 kcal/mol). By comparison, ketanserin (SD) (-27.55 kcal/mol) and pimavanserin (SD) (+4.08 kcal/mol) showed poor energetics. These findings identify Desmodin and 5,7,2′,4′-Tetrahydroxy-6-prenylisoflavanone as promising MAO-B inhibitors, and Desmodin and N, N-Dimethyltryptamine as the most potent 5-HT2A binders, with stability at both targets and favourable energetics. They also align with conventional in silico drug design principles where MM-GBSA is used to improve docking scores to better rank ligands and evaluate their stability in MAO-B studies (Iwaloye *et al.,* 2020; Ajala *et al.,* 2024).

We also used AutoQSAR modeling to develop predictive models for the two targets based on ChEMBL inhibitor data. For MAO-B, 52 inhibitors were split into 41 training compounds (≈80%) and 11 test compounds (≈20%) with observed and predicted pIC50 values reported in Table 10. The top model, kpls_linear_49, with R^2 of 0.8404, Root Mean Square Error (RMSE) of 0.6042, and Q^2 of 0.7567 (Table 9) confirmed the model's predictive capacity. For 5-HT2A, 72 inhibitors were divided into 55 training compounds (≈76%) and 17 test compounds (≈24%), with observed and predicted pIC50 values given in Table 12. The top-performing model, kpls_linear_5, had R^2 0.8916, RMSE 0.2997, and Q^2 0.9046 (Table 11), with an even better fit. In both models, the error was typically within ±1 log unit, and these models were then used to predict the bioactivity of the compounds. These results demonstrate the effectiveness of AutoQSAR for predicting the bioactivity of ligands from curated ChEMBL data, with internal validation metrics (R^2, Q^2, RMSE) supporting the use of the model for profiling MAO-B and 5-HT2A inhibitors for virtual screening (Alves *et al.,* 2025; Iwaloye *et al.,* 2020; Zhang *et al.,* 2025).

MD simulations dynamically validated the stability of ligand–protein interactions. MAO-B bound to ligand Desmodin, 5,7,2′,4′-Tetrahydroxy-6-prenylisoflavanone, and positive control rasagiline (SD) was simulated for 100 ns to assess stability and dynamic changes. RMSD values revealed that the apo-protein and rasagiline complex were stable within the acceptable range of 1-4.5 nm, whereas Desmodin and the prenylated isoflavanone showed slight fluctuations (40-100 ns) before forming stable complexes. This suggests that the presence of ligands caused conformational changes but eventually led to increased rigidity and stability of the protein. RMSF analysis showed less flexibility in the active site residues in the ligand-bound states compared to apo, with fluctuations confined to loop regions, indicating that the active site was stabilized. The radius of gyration showed stability for all systems, indicating that the overall compactness of the protein was maintained. Hydrogen bond analysis showed consistent interactions along the trajectory, confirming the stability of the complexes. The SASA slightly decreased in the presence of the ligands, reflecting enhanced packing and reduced solvent exposure. Ramachandran plots also revealed that most residues were in preferred areas, highlighting the stability of the complexes. These results are

supported by the MD trajectories presented in Figures 7–9, while structural stability assessments from Ramachandran analysis and RMSD comparisons are shown in Figures 10 and 11. Overall, these results confirm that Desmodin and the prenylated isoflavanone bind stably to MAO-B, similar to the known inhibitor rasagiline; hence, they could be safe and effective MAO-B inhibitors. Following the principles of molecular dynamics in structure-based drug design, the assessment of RMSD, RMSF, Rg, SASA, and hydrogen bond interactions offers compelling evidence of protein-ligand complex stabilization by ligand binding (Nandana *et al.,* 2025; Alves *et al.,* 2025; Ajala *et al.,* 2024).

Conclusion

This study offers a thorough in-silico evaluation of the *Desmodium gangeticum* phytochemicals as prospective modulators of MAO-B and 5-HT2A, two clinically overlapping therapeutic targets in PD. The main therapeutic target was MAO-B inhibition, which is crucial to restore dopamine tone and improve motor symptoms. Though, traditional MAO-B inhibitors worsen hallucinations and psychosis, as a result of dopamine-serotonin imbalance in PD. Intriguingly, some of the phytochemicals from *D. gangeticum* not only have superior binding, stability, and pharmacokinetics at MAO-B than rasagiline, but also have high antagonistic potential at 5-HT2A, the serotonin receptor most associated with PD-related hallucinations. This dual mechanism provides a rational approach to addressing the therapeutic conundrum in PD by relieving motor symptoms without aggravating neuropsychiatric symptoms. After docking, MM-GBSA energetics, ADMET profiling, QSAR validation, and molecular dynamics simulations, Desmodin, 5,7,2′,4′-Tetrahydroxy-6-prenylisoflavanone, N, N-Dimethyltryptamine, and Tryptamine emerge as lead candidates with optimal efficacy and safety. Overall, these results herald *D. gangeticum* metabolites as promising dual markers for further experimental testing as safer agents that can potentially alleviate both motor and non-motor PD symptoms.

Challenges and Limitations

In this study, we provide extensive in-silico evidence that *Desmodium gangeticum* phytochemicals are potential dual modulators of MAO-B and 5-HT2A receptors; however, there are limitations. First, while compounds like Desmodin and 5,7,2′,4′-Tetrahydroxy-6-prenylisoflavanone showed the best docking scores and MM-GBSA binding energies, their predicted pIC_{50} values were not as high as the synthetic inhibitor, suggesting further optimization might be required to improve potency. Toxicity predictions also indicated moderate LD_{50} values for some phytochemicals (e.g., Kievitone at 10 mg/kg), suggesting that they may pose safety issues that need to be addressed experimentally.

A further limitation is the use of computer predictions. While docking, QSAR and MD simulations offer useful insights into mechanisms, they cannot completely mimic biological interactions. For instance, AutoQSAR models with ChEMBL inhibitors provided high R^2 and Q^2 values, but the residue errors of ±1 log unit suggest variability that may affect in vivo activity. Additionally, while the MD simulations confirmed stability, they were only run for 100 ns and only included MAO-B, not 5-HT2A complexes.

Potential solutions to counter this include nanoformulations, lipid formulations, or prodrugs to improve solubility and intestinal permeability of non-compliant compounds. Medicinal chemistry optimisation can enhance potency and minimise toxicity, whereas longer MD simulations and the inclusion of 5-HT2A complexes will offer a more comprehensive view of the dynamics. Critically, in vitro studies using enzymatic and cellular models are needed to ensure the predicted dual-target efficacy and safety are validated.

Future Directions and Clinical Translation

The compounds: Desmodin, 5,7,2′,4′-Tetrahydroxy-6-prenylisoflavanone, N, N-Dimethyltryptamine, and Tryptamine, have promising interactions predicted with MAO-B and 5-HT2A, and could potentially be used as dual modulators for the treatment of Parkinson's disease. The next phase is to experimentally confirm the interactions with MAO-B and 5-HT2A by enzymatic studies. If confirmed, subsequent experiments should evaluate activity in dopaminergic and serotonergic cells, in vivo pharmacokinetics, and consider approaches to improve bioavailability, selectivity and safety. Structural optimisation

may be required to enhance activity, and formulation strategies such as nanotechnology or prodrugs may be needed to improve solubility and permeability.

Finally, to move towards clinical utility, efficacy should be examined in animal models of Parkinson's disease and subsequent clinical trials should be conducted to determine therapeutic benefits and safety in humans. Through dual modulation of motor and non-motor features, these phytochemicals may offer a safer and more well-rounded therapy that directly addresses the dopamine-serotonin paradox that exists in current therapies.

Author contributions

O.E. Akinma: Conceptualization, methodology, investigation, formal analysis, and writing – original draft.
O.A. Akinola: Supervision, investigation, validation, formal analysis, and writing – review & editing.
I.D. Ojo: Methodology, investigation, formal analysis, and writing – original draft preparation.
A.I. Olopoda: Investigation, validation, writing – original draft, analysis and visualization, and writing – review & editing.
I.D. Akerele: Methodology, formal analysis and investigation.
B.B. Akinyemi: Methodology and investigation.
F.O. Ayodeji: Methodology and investigation.
O.O. Elekofehinti: Conceptualization, supervision and resources
All authors reviewed and approved the final manuscript.

Funding
No funding was received for conducting this study.

Competing Interests
The authors declare no competing interests.

References

1. Ajala A, Eltayb WA, Abatyough TM, et al. 2024. In-silico screening and ADMET evaluation of therapeutic MAO-B inhibitors against Parkinson disease. *Intelligent Pharmacy* 2:554–564.
2. Alborghetti M, Bianchini E, De Carolis L, et al. 2023. Type-B monoamine oxidase inhibitors in neurological diseases: clinical applications based on preclinical findings. *Neural Regeneration Research* 19:16–21. https://doi.org/10.4103/1673-5374.375299
3. Alves PA, Camargo LC, Souza GMD, Mortari MR, Homem-de-Mello M. 2025. Computational modeling of pharmaceuticals with an emphasis on crossing the blood–brain barrier. *Pharmaceuticals* 18:217. https://doi.org/10.3390/ph18020217
4. Banerjee P, Kemmler E, Dunkel M, Preissner R. 2024. ProTox 3.0: a webserver for the prediction of toxicity of chemicals. *Nucleic Acids Research* 52:W513–W520. https://doi.org/10.1093/nar/gkae303
5. Bora M, Mandal S, Singh P, et al. 2023. Phytochemical and pharmacological profile of *Desmodium gangeticum* (L.) DC.: a comprehensive review. *Current Traditional Medicine* 9:e050523217381. https://doi.org/10.2174/2215083810666230523145738
6. Chang HC, Lien J, Hsueh MC, Wu CR. 2024. Exploring the neuroprotective potential of *Desmodium* species: insights into radical scavenging capacity and mechanisms against 6-OHDA-induced neurotoxicity. *Plants* 13:1742. https://doi.org/10.3390/plants13131742

7. Cherkasov A, Muratov EN, Fourches D, et al. 2024. Best practices for QSAR model development and validation in the era of machine learning. *Journal of Chemical Information and Modeling* 64:1285–1310. https://doi.org/10.1021/acs.jcim.3c01526

8. Cummings J, Lanctôt K, Grossberg G, Ballard C. 2024. Progress in pharmacologic management of neuropsychiatric syndromes in neurodegenerative disorders: a review. *JAMA Neurology* 81:645–660. https://doi.org/10.1001/jamaneurol.2024.0586

9. de Bie RMA, Katzenschlager R, Swinnen B, et al. 2025. Update on treatments for Parkinson's disease motor fluctuations – an International Parkinson and Movement Disorder Society evidence-based medicine review. *Movement Disorders* 40:403–425. https://doi.org/10.1002/mds.30162

10. de Lima EP, Laurindo LF, Catharin VCS, et al. 2025. Polyphenols, alkaloids, and terpenoids against neurodegeneration: evaluating the neuroprotective effects of phytocompounds. *Metabolites* 15:124. https://doi.org/10.3390/metabo15020124

11. Di Biase L, Pecoraro PM, Carbone SP, et al. 2023. Levodopa-induced dyskinesias in Parkinson's disease: an overview on pathophysiology and therapy. *Journal of Clinical Medicine* 12:4427. https://doi.org/10.3390/jcm12134427

12. Fakhri S, Iranpanah A, Gravandi M, et al. 2021. Natural products attenuate PI3K/Akt/mTOR signaling pathway: a promising strategy in neurodegeneration. *Phytomedicine* 91:153664. https://doi.org/10.1016/j.phymed.2021.153664

13. Genheden S, Ryde U. 2021. The MM/PBSA and MM/GBSA methods to estimate ligand-binding affinities. *Expert Opinion on Drug Discovery* 10:449–461.

14. Iwaloye O, Elekofehinti OO, Momoh AI, Babatomiwa K, Ariyo EO. 2020. In silico molecular studies of natural compounds as possible anti-Alzheimer's agents: ligand-based design. *Network Modeling Analysis in Health Informatics and Bioinformatics* 9:54.

15. Johnston RC, Yao K, Kaplan Z, et al. 2023. Epik: pKa and protonation state prediction through machine learning. *Journal of Chemical Theory and Computation* 19:2380–2388.

16. Jost W. 2022. A critical appraisal of MAO-B inhibitors in the treatment of Parkinson's disease. *Journal of Neural Transmission* 129:723–736. https://doi.org/10.1007/s00702-022-02465-w

17. Kossatz E, Diez-Alarcia R, Gaitonde SA, et al. 2024. G protein-specific mechanisms in the serotonin 5-HT2A receptor regulate psychosis-related effects. *Nature Communications* 15:4046. https://doi.org/10.1038/s41467-024-48196-2

18. Kwan C, Frouni I, Nuara SG, et al. 2021. Combined 5-HT2A and mGlu2 modulation for Parkinson's disease psychosis. *Neuropharmacology* 186:108465. https://doi.org/10.1016/j.neuropharm.2021.108465

19. Lee H, Kim J, Kim JW, Lee Y. 2025. Recent advances in AI-based toxicity prediction for drug discovery. *Frontiers in Chemistry* 13:1632046. https://doi.org/10.3389/fchem.2025.1632046

20. Lu C, Wu C, Ghoreishi D, et al. 2021. OPLS4: improving force field accuracy. *Journal of Chemical Theory and Computation* 17:4291–4300.

21. Merghany RM, El-Sawi SA, Aboul Naser AF, et al. 2025. Pelargonium graveolens attenuates rotenone-induced Parkinson's disease. *Molecular Neurobiology* 62:7664–7681. https://doi.org/10.1007/s12035-025-04727-6

22. Mohan PK, Adarsh Krishna TP, Senthil Kumar T, Ranjitha Kumari B. 2021. Pharmacochemical profiling of *Desmodium gangeticum*. *Future Journal of Pharmaceutical Sciences* 7:206. https://doi.org/10.1186/s43094-021-00356-7

23. Mohanraj K, Santhosh RS, Vivek-Ananth RP, et al. 2022. IMPPAT 2.0: phytochemical atlas of Indian medicinal plants. *ACS Omega* 7:7136–7149.

24. Nandana RK, Niraimathi SR, Happuch SSK, et al. 2025. In silico analysis of *Tecomella undulata* in Parkinson's disease. *Journal of Bio-X Research* 8:0054. https://doi.org/10.34133/jbioxresearch.0054

25. Ojo ID, Olusanya MD, Oyelere TE, et al. 2025. In silico identification of CDK1 as a therapeutic target in breast cancer. *Discover Chemistry* 2:Article 1. https://doi.org/10.1007/s44371-025-00405-7

26. Pirker W, Ferreira JJ, Rascol O, Poewe W. 2026. Management of Parkinson's disease psychosis. *The Lancet Regional Health – Europe* 62.

27. Rahman R, Bajgai J, Fadriquela A, et al. 2021. Therapeutic potential of natural products in neurodegenerative disorders. *Molecules* 26:5327. https://doi.org/10.3390/molecules26175327

28. Ramírez D, Caballero J. 2016. Molecular docking reliability for enantiomer pairs. *International Journal of Molecular Sciences* 17:525. https://doi.org/10.3390/ijms17040525

29. Rani ML, Kumar RD, Indumathy V, et al. 2022. Molecular docking of *Desmodium gangeticum* against MAO-B. *NeuroQuantology* 20:11548–11560.

30. Roos K, Wu C, Damm W, et al. 2021. OPLS4 force field improvements. *Journal of Chemical Information and Modeling* 61:4521–4536. https://doi.org/10.1021/acs.jcim.1c00591

31. Sastry GM, Adzhigirey M, Day T, Annabhimolu R, Sherman W. 2021. Protein and ligand preparation protocols. *Journal of Computer-Aided Molecular Design* 35:261–278. https://doi.org/10.1007/s10822-020-00363-5

32. Schiess N, Cataldi R, Okun MS, et al. 2022. Global disparities in Parkinson disease. *JAMA Neurology* 79:929–936. https://doi.org/10.1001/jamaneurol.2022.1783

33. Schneider LS. 2022. Safety of pimavanserin in Parkinson's disease. *American Journal of Psychiatry* 179:531–535. https://doi.org/10.1176/appi.ajp.20220519

34. Schrödinger LLC. 2021. Maestro, version 12.8. New York: Schrödinger.

35. Segal GS, Xie SJ, Paracha S, Grossberg G. 2021. Psychosis in Parkinson's disease. *Journal of Geriatric Psychiatry and Neurology* 34:280–287. https://doi.org/10.1177/08919887211018280

36. Sharifi-Rad J, Rapposelli S, Sestito S, et al. 2022. Multitarget phytochemicals in Alzheimer's disease. *Journal of Personalized Medicine* 12:1515. https://doi.org/10.3390/jpm12091515

37. Shruti S, Bharadvaja N. 2024. In silico identification of plant compounds in Parkinson's disease. *Letters in Applied NanoBioScience* 13:78.

38. Singh A, Sinha S, Singh NK. 2024. Dietary flavonoids targeting MAO-B. *Chemical Biology & Drug Design* 104:e14619.

39. Su D, Cui YL, He C, et al. 2025. Global projections of Parkinson's disease. *BMJ* 388:e080952. https://doi.org/10.1136/bmj-2024-080952

40. Tan YY, Jenner P, Chen S. 2021. MAO-B inhibitors in Parkinson's disease. *Journal of Parkinson's Disease* 11:1007–1023. https://doi.org/10.3233/JPD-212976

41. Tariot P, Cummings J, Soto-Martin M, et al. 2021. Pimavanserin trial in dementia-related psychosis. *New England Journal of Medicine* 385:309–319. https://doi.org/10.1056/NEJMoa2034634

42. Torres-Yaghi Y, Carwin A, Carolan JF, et al. 2021. QTc prolongation in Parkinson's therapies. *Neuropsychiatric Disease and Treatment* 17:3791–3818. https://doi.org/10.2147/NDT.S324145

43. Vemula D, Jayasurya P, Sushmitha V, et al. 2022. AI in drug discovery. *European Journal of Pharmaceutical Sciences* 181:106324. https://doi.org/10.1016/j.ejps.2022.106324

44. Zhang J, Li H, Zhang Y, et al. 2025. Computational toxicology using AI. *Briefings in Bioinformatics* 26:bbaf533. https://doi.org/10.1093/bib/bbaf533

45. Zhong Q, Zhu F. 2022. Parkinson's disease burden trends. *Neuroepidemiology* 56:261–270. https://doi.org/10.1159/000524208